HHS Public Access

Author manuscript

Clin Cancer Res. Author manuscript; available in PMC 2016 March 15.

Published in final edited form as:

Clin Cancer Res. 2015 March 15; 21(6): 1340–1347. doi:10.1158/1078-0432.CCR-14-1178.

Pharmacodynamic imaging guides dosing of a selective estrogen receptor degrader

Pedram Heidari[1], **Francis Deng**[1,2], **Shadi A. Esfahani**[1], **Alicia K. Leece**[1], **Timothy M. Shoup**[3], **Neil Vasdev**[3], and **Umar Mahmood**[1,*]

[1]Athinoula A. Martinos Center for Biomedical Imaging, Department of Radiology, Massachusetts General Hospital, Boston, MA

[2]Washington University School of Medicine, St. Louis, MO

[3]Division of Nuclear Medicine and Molecular Imaging, Department of Radiology, Massachusetts General Hospital, Boston, MA

Abstract

Purpose—Estrogen receptor (ER) targeting is key in management of receptor-positive breast cancer (BrCa). Currently, there are no methods to optimize anti-ER therapy dosing. This study assesses the utility of 16α-^{18}F-fluoroestradiol (^{18}F-FES) PET for fulvestrant dose optimization in a preclinical ER+ BrCa model.

Experimental Design—In vitro, ^{18}F-FES retention was compared to ERα protein expression (ELISA) and *ESR1* mRNA transcription (qPCR) in MCF7 cells (ER+) after treatment with different fulvestrant doses. MCF7 xenografts were grown in ovariectomized nude mice and assigned to vehicle, low- (0.05mg), medium- (0.5mg) or high-dose (5mg) fulvestrant treatment groups (5–7 per group). Two and three days after fulvestrant treatment, PET/CT was performed using ^{18}F-FES and ^{18}F-FDG, respectively. ER expression was assessed by immunohistochemistry, ELISA, and qPCR on xenografts. Tumor proliferation was assessed using Ki-67 immunohistochemistry.

Results—In vitro, we observed a parallel graded reduction in ^{18}F-FES uptake and ER expression with increased fulvestrant doses, despite enhancement of ER mRNA transcription. In xenografts, ER expression significantly decreased with increased fulvestrant dose, despite similar mRNA expression and Ki-67 staining among the treatment groups. We observed a significant dose-dependent reduction of ^{18}F-FES PET mean standardized uptake value (SUV_{mean}) with fulvestrant treatment, but no significant difference among the treatment groups in ^{18}F-FDG PET $SUV_{mean.}$.

Conclusion—We demonstrated that ^{18}F-FES uptake mirrors the dose-dependent changes in functional ER expression with fulvestrant resulting in ER degradation and/or blockade; these precede changes in tumor metabolism and proliferation. Quantitative ^{18}F-FES PET may be useful for tracking early efficacy of ER blockade/degradation and guiding ER-targeted therapy dosing in BrCa patients.

*Correspondence to: Umar Mahmood, M.D., Ph.D., Athinoula A. Martinos Center for Biomedical Imaging, Department of Radiology, Massachusetts General Hospital, Boston, MA 02114, Tel: 617-726-6477, Fax: 617-726-6165, umahmood@mgh.harvard.edu.

Conflict of interest: The authors declare that there are no conflicts of interest

Keywords

Positron Emission Tomography; ^{18}F-Fluoroestradiol; Breast Cancer; Fulvestrant; Optimal biological dose

INTRODUCTION

Estrogen receptor-α (ERα) is expressed in the majority of human breast cancers (BrCa) and is a critical driver of breast tumorigenesis (1, 2). Therefore, expression of ERα is an important factor in prediction of prognosis and effectiveness of anti-hormone therapy. Patients with ERα-positive (ERα+) tumors typically have longer overall survival and are more likely to respond to hormone-targeted therapies (3). The expression of ERα is highly variable among BrCa patients and moreover, there is a high degree of heterogeneity found in the level of ERα expression among the metastatic foci in individual patients (4, 5).

Selective estrogen receptor down-regulators (SERDs) are a relatively new class of drugs for the treatment of ER-expressing BrCa. Fulvestrant, the prototypical SERD, competitively binds ER, disrupts nuclear uptake of ER, and accelerates receptor turnover via the ubiquitin-proteasome pathway (6–8). Fulvestrant is currently indicated for the treatment of metastatic breast cancer in postmenopausal women. While its efficacy is well-established in first- and second-line settings, only a fraction of women treated with fulvestrant experience an objective response (9–11). Some hypothesized that the approved dose was suboptimal, spurring trials of different dosing regimens (12). While limited studies have demonstrated that fulvestrant-induced ER downregulation is dose-dependent, (13, 14) the foray into high-dose regimens proceeded empirically, with a deduced assumption of the level of ER downregulation with fulvestrant therapy and how ER level changes over the course of monthly treatment cycles (15–18). The development of a non-invasive approach to quantify early pharmacodynamic effects would facilitate dose optimization at both the individual and treatment population levels.

Molecular imaging modalities, such as positron emission tomography (PET), permit early evaluation of tumor biology and assessment of treatment response, well before tumor morphology or histopathology changes occur (19). The estrogen-based radiopharmaceutical ^{18}F-fluoroestradiol (^{18}F-FES) is a PET imaging agent that has high binding affinity and selectivity for the ERα subtype and has been shown to exhibit high specific uptake by ER-rich target tissues and ERα-positive mammary tumors (20–22). The agent focally accumulates at sites of specific overexpression of ERα. The use of ^{18}F-FES PET as a measure of tumoral ERα expression has been validated in clinical studies (20, 23, 24). ^{18}F-FES imaging, in limited studies, has been shown to be of value in prediction of responsiveness to anti-hormone therapy (25–28). This radiotracer can be utilized to quantitate the ERα density in BrCa (24, 27) and therefore can be used to precisely monitor the effects of any drug that abolishes ERα production, promotes ERα degradation, or that competes with ^{18}F-FES for ERα binding (29)(Fig. 1). Thus, ^{18}F-FES PET imaging provides an unprecedented opportunity to assess immediate drug efficacy on ER capacity and guide dose selection in individual patients.

The objective in this study was to use the quantitative nature of ^{18}F-FES PET imaging to monitor the ER that is occupied and/or degraded by fulvestrant (SERD) treatment at a given time, based on changes in the levels of available receptor for ^{18}F-FES binding. Using another PET radiotracer, ^{18}F-fluoro-deoxy-glucose (^{18}F-FDG), and a histopathological biomarker of proliferation (Ki-67), we were able to demonstrate the advantage of ERα imaging for early assessment of therapy well before the metabolic and histopathologic effects of treatment can be observed. The concept of ERα imaging for individualized dose adjustment early in the course of treatment has the potential to be readily translated to patients with BrCa to more effectively monitor treatment and improve dosing regimens.

METHODS

Radiopharmaceuticals

^{18}F-FDG was purchased from IBA Molecular (Haverhill, MA). 16α-^{18}F-FES was synthesized according to the literature (30). The mean specific activity of ^{18}F-FES used in this study was 6.1Ci/μmol (range: 5.4–6.8 Ci/μmol).

Cell culture

Cell lines and culture media were obtained from ATCC (Manassas, VA). The ER-expressing human breast adenocarcinoma cell line**,** MCF-7, and triple negative human breast adenocarcinoma line, MDA-MB-231, were grown in Dulbecco's Modified Eagle's Medium (DMEM) and Leibovitz's L-15 Medium, respectively. Both media were supplemented with 10% fetal bovine serum (Atlanta Biologicals, Norcross, GA) and 1% penicillin-streptomycin (Gibco, Life Technologies, Grand Island, NY). All cells were maintained in a humidified incubator at 37°C with 5% CO_2. The cells were in culture for less than 6 months after resuscitation. Cell lines undergo comprehensive quality control and authentication procedures by ATCC before shipment. These include testing for mycoplasma by culture isolation, Hoechst DNA staining, and PCR, together with culture testing for contaminant bacteria, yeast, and fungi. Authentication procedures used include species verification by DNA barcoding and identity verification by DNA profiling.

In-vitro ^{18}F-FES retention with variable dose fulvestrant treatment

MCF-7 cells were seeded in 24-well plates at 5×10^4 cells per well and were allowed to grow and attach for 24 hours. The sub-confluent cultures were serum-starved and incubated for 24 hours with fulvestrant (10^{-12} to 10^{-6} mol/L; Sigma-Aldrich, St. Louis, MO) or vehicle only (0.1% dimethylsulfoxide (Sigma-Aldrich, St. Louis, MO) in base culture medium) in triplicate. Each well was incubated with 25 μCi ^{18}F-FES in the same formulation of treatment medium as before, for 30 min at 37°C. Wells were gently washed three times in cold Hank's Balanced Salt Solution (HBSS; Fisher Scientific, Pittsburg, PA), trypsinized, and transferred to counting tubes. Radiotracer uptake was quantified using a gamma counter (WIZARD2; PerkinElmer, Waltham, MA). Total counts per well were corrected for decay and normalized by defining the maximum uptake group as 100% and non-specific uptake by vehicle-treated MDA-MB-231 cells as 0%.

Cellular ER expression and ESR1 mRNA concentration

MCF-7 cells were plated in 6-well plates at 2.5×10^5 cells per well. The sub-confluent cultures were serum-starved for a day and then incubated for 24 hours with fulvestrant (10^{-12} to 10^{-6} mol/L) or vehicle. Wells were washed with Dulbecco's Phosphate Buffered Saline–without calcium (Fisher Scientific, Pittsburg, PA) and trypsinized. Using a PARIS Kit (Ambion, Life Technologies, Grand Island, NY), cellular extract was fractionated into nuclear and cytoplasmic fractions. Absolute nuclear protein concentration was quantified by micro BCA assay (Pierce, Thermo Fisher Scientific Inc., Rockford, IL) against a bovine serum albumin standard curve, and RNA was quantitated using a ND-1000 spectrophotometer (NanoDrop Wilmington, DE). Intra-sample coefficient of variation of total nuclear protein content was 12.7% (n=9), indicating relatively little effect of brief fulvestrant treatment on cellularity.

Relative ERα protein expression was measured by sandwich enzyme-linked immunosorbent assay (ELISA; Active Motif, Carlsbad, CA) using 5 μg nuclear extract per well. Results are reference (600 nm) wavelength-subtracted absorbance, normalized by defining the maximum expression group as 100% and non-specific binding by nuclear lysate from MDA-MB-231 cells as 0%. Technical ELISA duplicates were averaged to derive values for biological replicates in independent experiments.

Relative *ESR1* mRNA concentration was measured by quantitative reverse transcription polymerase chain reaction (qRT-PCR). In independent culture experiments, 36 ng or 200 ng total RNA was used for reverse transcription (High Capacity RNA-to-cDNA kit; Life Technologies, Grand Island, NY). Out of the 20 μl cDNA reaction volume for each sample, 4.5 μl was used for Taqman gene expression assay reaction for human *ESR1* (Hs00174860_m1) and *GAPDH* endogenous control (Life Technologies, Grand Island, NY). Thermocycling was conducted on a 7500 Fast Real-Time PCR system (Applied Biosystems, Life Technologies, Grand Island, NY). Cycle thresholds (Ct) were set automatically in SDS software (version 1.4; Applied Biosystems) and normalized by subtracting the Ct value for *GAPDH* from that of *ESR1* (denoted as ΔCt). Results were reported as ΔCt so that values relate directly with the logarithm of target mRNA concentrations.

Tumor implantation and treatment

Female athymic nude mice (6–8 weeks old) were obtained from Charles River Laboratories (Wilmington, MA). Animal protocols were approved by the Subcommittee on Research Animal Care at Massachusetts General Hospital. In order to reduce competition from the endogenous estradiol all the mice were ovariectomized at least one week prior to tumor implantation. We used intermittent estradiol dosing to minimize competition with radiotracer at the time of imaging. Mice were supplemented with daily subcutaneous injections of 17β-estradiol (Abcam, Cambridge, MA) (20 μg in 20 μl sesame oil:ethanol [9:1; v:v]) beginning at least three days prior to tumor implantation (31). MCF7 cultures were harvested and resuspended 1:1 (v:v) in Matrigel (BD Biosciences, San Jose, CA). Approximately 5×10^6 cells in 100 μl were injected subcutaneously over the right upper flank. Tumor growth was monitored by caliper measurements along two perpendicular axes.

When tumors grew to approximately 5 mm in diameter, mice were randomly allocated to treatment groups.

At treatment time, estradiol supplementation was withdrawn. Mice received one subcutaneous injection of fulvestrant (0.05 mg, 0.5 mg, or 5 mg) or vehicle (100 μl sesame oil:ethanol [9:1; v:v]). Two days following treatment, mice were either imaged with ^{18}F-FES and ^{18}F-FDG or euthanized to harvest the tumor for *in vitro* analyses. Caliper-measured tumor size did not change significantly between treatment and analysis time points. Across all analyzed mice, average two dimensional tumor size measurements using a caliper were 6.42 ± 1.44 x 4.95 ± 0.70 mm (mean ± SD) at treatment time. The tumor dimensions were 6.98 ± 1.61 x 5 ± 1.16 mm, 6.36 ± 2.33 x 4.63 ± 0.81 mm, 6.28 ± 0.60 x 5.16 ± 0.20 mm, and 6.45 ± 1.40 x 5.08 ± 0.42 mm in the vehicle, low-dose (0.05 mg), medium-dose (0.5 mg) and high-dose (0.05 mg) groups, respectively. Tumor volumes as measured on computed tomography (CT) were on average 72 ± 18 mm^3.

Tumor ER expression assays

Extracted xenografts (3 per group) were immersed in ice-cold cellular lysis buffer from the PARIS Kit and disrupted using a rotor-stator homogenizer. Relative ERα protein expression was measured on sandwich ELISA using 20 μg whole cell lysate per well. Non-specific absorbance from a reference wavelength and from diluent-only control were subtracted. RNA was purified from a fraction of the lysate immediately after homogenization and reverse transcription was performed on 150 ng total cellular RNA. qRT-PCR and data processing were performed as described above.

Part of the resected tumor was fixed in 10% neutral buffered formalin for 24 hours and embedded in paraffin. Serial sections in 4 μm-thick slices were used for immunohistochemistry (IHC). For ER assessment, slides underwent heat-induced epitope retrieval (HIER) using citrate-based (pH 6.0) buffer for 15 minutes heated to a maximum of 99°C, followed by incubation with prediluted monoclonal antibody 6F11 (Abcam, Cambridge, MA) (approximately 10 mg/ml). For Ki-67 assessment, separate slides underwent HIER using EDTA-based (pH 9.0) buffer for 20 minutes at 99°C, followed by incubation with monoclonal antibody MIB-1 (Abcam, Cambridge, MA) (1:200). All primary antibodies were incubated for 15 minutes at room temperature and detected using a polymer-based DAB system (Thermo Fisher Scientific Inc., Rockford, IL). Photomicrographs were recorded using the Olympus IX51 microscope equipped with a DP72 camera under consistent magnification (20x), exposure duration, and lighting.

Small-animal PET

For ^{18}F-FDG-PET only, animals were fasted for at least 4 hours prior to radiotracer injection. ^{18}F-FES and ^{18}F-FDG were respectively injected two and three days after treatment (5–6 mice per treatment group) via a 30-gauge catheter introduced in the lateral tail vein. Actual activities injected, calibrated to time of scan, were 9.7 ± 2.2 MBq (263 ± 59 μCi; mean, SD) of ^{18}F-FES and 9.9 ± 1.7 MBq (268 ± 45 μCi) of ^{18}F-FDG. Actual times elapsed between injection and PET acquisition were 69 ± 12 min (FES) and 69 ± 7 min (FDG). PET data were acquired under a whole-body emission protocol on an Argus small-

animal PET/CT scanner (Sedecal, Madrid, Spain) for 15 min in 2 bed positions. Images were reconstructed with a 2D ordered-subset expectation maximization (2D-OSEM) algorithm. CT data were acquired in 100-μm resolution. The scans were acquired with tube voltage of 40 kVp, and tube current of 140 μA. Total scan duration was approximately 14 minutes. Image data were reconstructed using the Feldkamp algorithm. Three-dimensional regions of interest (ROI) were manually drawn around tumors based on co-registered PET/CT scans. Mean standardized uptake values (SUV_{mean}) were calculated within the ROI. ^{18}F-FES SUV_{mean} was also normalized to blood pool activity at the time of scan from a 3D spherical 3 mm ROI drawn within the heart and ^{18}F-FES uptake was expressed as target-to-background ratio (TBR).

Statistical analyses

Statistical analysis was performed with Prism software (version 5; GraphPad, La Jolla, CA). Data from multiple groups were compared by one-way analysis of variance (ANOVA) followed by Holm-Sidak's post hoc multiple comparisons test. For in vitro experiments only, semi-logarithmic dose-response data were fit to four-parameter sigmoidal curves. Correlation analysis was conducted using Pearson's r. Data are graphed as mean ± standard error of the mean. *P* values less than 0.05, multiplicity-adjusted when appropriate, were considered significant.

RESULTS

In vitro analysis of MCF7 cells

We performed ^{18}F-FES retention studies after incubating MCF7 cells with serial dilution doses of fulvestrant for 24 hours. Significant dose-dependent changes in ^{18}F-FES uptake were observed (Fig. 2A). The 50% inhibitory concentration (IC_{50}) was 8.2 nmol/L (95% CI: $3.5x10^{-10}$ to 1.9×10^{-7} mol/L; model R square: 0.834). Compared to vehicle control, specific ^{18}F-FES retention decreased significantly by 48.5% (p=0.03), 53.1% (p=0.02), 79.7% (p<0.001), and 85.7% (p<0.001) when the cells were treated with 1, 10, 100, and 1000 nmol/L fulvestrant, respectively.

To assess whether changes in ^{18}F-FES uptake could be attributed to competitive binding with fulvestrant or changes in total receptor concentration, we determined ERα protein expression in cells treated in parallel. Dose-dependent changes in ERα protein levels were observed (Fig. 2B). The IC_{50} was 4.4 nmol/L (95% CI: 3.0×10^{-10} to 6.4×10^{-8} mol/L; model R square: 0.613), a potency similar to that observed by ^{18}F-FES uptake. However, the ERα expression down-regulation in MCF7 cells paralleled the reduction seen with ^{18}F-FES uptake with fulvestrant treatment.

To account for upstream changes in gene expression, we measured the level of *ESR1* mRNA transcripts following treatment. Fulvestrant induced a dose-dependent increase in *ESR1* expression (Fig. 2C; approximately three-fold), possibly reflecting negative feedback loop relief. The 50% effective concentration was 0.17 nmol/L (95% CI: 1.8×10^{-11} to 1.6×10^{-9} mol/L; model R square: 0.596). These data suggest that, in breast cancer cells *in vitro*,

fulvestrant down-regulates ER specifically at the protein level, a dose-dependent change that is captured by ^{18}F-FES uptake.

Ex vivo analysis of tumor xenografts

In MCF7 xenografts resected 48 h after fulvestrant treatment, nuclear ERα protein expression displayed significant dose-dependent changes with fulvestrant treatment (Fig. 3A; p=0.001). Compared to vehicle, tumor ERα protein levels decreased by 30.6% (p=0.03), 73.9% (p=0.0015), and 74.9% (p=0.0015) when mice were treated with 0.05 mg, 0.5 mg, and 5 mg fulvestrant, respectively. These changes in protein expression from tumor lysate were confirmed by ER IHC. Qualitative analysis revealed reduced nuclear ER staining intensity and proportion of positive cells in tumors from mice treated with higher fulvestrant doses (Fig. 4A–D).

Upstream of ER protein expression, dose-dependent changes in *ESR1* mRNA expression were not apparent (Fig. 3B; p=0.39). Similarly, treatment was not associated with discernible reductions in staining for the proliferation marker Ki-67 (Fig. 4E–H). Most cells in non-necrotic areas of all tumors remained highly positive for Ki-67, indicating little effect on downstream ER function. Together, these data confirm that fulvestrant degrades ER specifically at the protein level in a dose-dependent manner *in vivo*, and that these changes occur prior to changes in proliferation.

In vivo PET imaging

We assessed whether quantitative molecular imaging with ^{18}F-FES demonstrates the dynamic range and sensitivity necessary to reveal early changes in fulvestrant-induced ER degradation/blockade at pharmacologic doses. Mean ^{18}F-FES PET SUV_{mean} in MCF7-xenografts was significantly different among groups 48 hours after fulvestrant treatment (Fig. 5A; p=0.0001). Tumor SUV_{mean} was 0.33± 0.02 for vehicle-treated mice and 0.33 ± 0.04 for low-dose (0.05 mg) fulvestrant-treated mice, which were not significantly different (p=0.86). However, compared to vehicle-treatment (control), fulvestrant treatment resulted in reduction of SUV_{mean} to 0.19 ± 0.03 (p=0.0054) at 0.5 mg and to 0.14 ± 0.02 (p=0.0006) at 5 mg doses. Compared to low-dose fulvestrant (0.05 mg), both 0.5 mg and 5 mg fulvestrant doses significantly reduced SUV_{mean} (p=0.009 and p=0.0011, respectively). There was no significant difference in ^{18}F-FES uptake between 0.5 mg and 5 mg treatment groups (p=0.33).

The target to background ratio (TBR) of MCF-7 xenografts in ^{18}F-FES PET imaging were 4.17 ± 0.41, 4.00 ± 0.62, 2.24 ± 0.30 and 1.49 ± 0.33 in the vehicle, 0.05 mg, 0.5 mg and 5 mg treatment groups, respectively. The difference in the mean TBR among different groups was significant (p=0.0005). The mean TBR was significantly lower in 0.5 mg and 5 mg dose groups than the vehicle control group (p=0.013 and p=0.0017, respectively). There was no significant difference in the mean TBR of 0.05 mg and vehicle treated groups (p=0.79) nor was there any difference in the mean TBR of 0.5 mg and 5 mg treatment groups (p=0.4).

Downstream metabolic changes were not evident three days after fulvestrant treatment. Mean SUV_{mean} of MCF-7 xenografts in ^{18}F-FDG PET imaging in the vehicle, 0.05 mg, 0.5

mg and 5 mg treatment groups were 1.40 ± 0.11, 1.50 ± 0.17, 1.47 ± 0.18 and 1.41 ± 0.09, respectively. There was no significant difference in SUV_{mean} among any of the dose groups in ^{18}F-FDG PET imaging (Fig. 5C; p=0.94). Representative images for all fulvestrant doses for both ^{18}F-FDG and ^{18}F-FES PET/CT are shown in Fig. 6.

There was no correlation between ^{18}F-FDG and ^{18}F-FES SUV_{mean} in MCF-7 xenografts (Fig. 5D; r=−0.038, R^2 =0.0014, p=0.89). The lack of correlation between ^{18}F-FES and ^{18}F-FDG PET imaging results is concordant with the histopathological analysis of xenograft samples in different treatment groups. The discrepancy between the two imaging sets suggests that changes in ERα availability occur much earlier than downstream effects on tumor metabolism and proliferation. Collectively, these data suggest that ^{18}F-FES-PET is able to interrogate fulvestrant-induced pharmacodynamic changes before other in vitro or in vivo biomarkers of treatment effectiveness.

DISCUSSION

Fulvestrant is approved by the FDA for treatment of ER positive metastatic BrCa in postmenopausal women with disease progression while on antiestrogen therapy. Despite the proven efficacy of fulvestrant, the optimal biological dose of this drug in BrCa treatment has been an area for debate. It is hypothesized that the lower than expected clinical performance of fulvestrant in BrCa may be explained by inadequate fulvestrant levels at standard recommended dosing levels, supported by recent reports of increased efficacy at higher doses (17, 32). Pooled analysis of clinical trials demonstrated an actual dose-dependent clinical response. The CONFIRM trial demonstrated that high dose fulvestrant (500 mg/month) produces a statistically significant and clinically relevant prolongation of progression-free survival (PFS) and duration of clinical benefit over a low-dose regimen (250mg/month), while the adverse effects profile remains essentially comparable with both dosing schemes (17, 18). ^{18}F-FES, an ER-specific radiotracer, has previously been employed for quantitative evaluation of ER expression in BrCa in clinical trials (21, 27, 29, 33, 34). Our findings support the ability of ^{18}F-FES PET to visualize the in vivo activity of endocrine therapy. In both in vitro and in vivo experiments, we demonstrated that ^{18}F-FES uptake in BrCa cells decreases in a dose-dependent manner in response to fulvestrant treatment. Our results are concordant with early findings in a retrospective study by Linden *et al*. that showed the incomplete tumor blockade of ^{18}F -FES uptake with fulvestrant may indicate a potential explanation for the lower-than-expected clinical performance of fulvestrant. (29). These findings have been recently confirmed in a prospective study, which demonstrated early progression of metastatic BrCa during in the first 3 months of fulvestrant therapy was related to significant residual ^{18}F-FES uptake (34). These findings match our findings and indicate that ^{18}F-FES may be used as a biomarker for fulvestrant efficacy and may help to identify patients that could potentially benefit from a higher dose.

To the best of our knowledge we have demonstrated for the first time that a graded response to fulvestrant can be monitored by ^{18}F-FES and the magnitude of reduction in radiotracer uptake was concordant with changes in functional ER expression. The reduction in ^{18}F-FES uptake by xenografts could be largely explained by reduced ER expression due to protein ubiquitination and degradation and/or direct blockade of ER by fulvestrant. We observed a

parallel but slightly greater reduction in ^{18}F-FES uptake than ER expression level changes with fulvestrant treatment. This suggests that the reduction in ^{18}F-FES uptake is mainly due to diminished ER expression, while direct blockade of ER by fulvestrant contributes to a considerably smaller part of the imaged change at the time point used in our study. Cancer cell apoptosis is a distant third possible minor cause for reduction in ^{18}F-FES uptake, given there was no change in proliferation, tumor size or ^{18}F-FDG uptake at the time of ^{18}F-FES PET imaging. In this regard, it is important to note that the alterations in ^{18}F-FES uptake by SERDs should to be cautiously attributed to changes in the ER expression. To further delineate the etiology of these effects, repeat tissue biopsy and/or multi-time point ^{18}F-FES PET imaging would provide additional insight.

We demonstrated ^{18}F-FES uptake highly correlated with ER protein levels but not mRNA expression. It has been shown that *ESR1* mRNA robustly correlates with protein expression and holds prognostic significance (35, 36). However, because SERD therapy uncouples ER protein expression from *ESR1* mRNA transcription by specifically degrading ER protein, ^{18}F-FES makes a better prognostic tool than *ESR1* mRNA for functional ER levels in the setting of such targeted therapy.

In this study we observed dissociation between dose-dependent reduction in ER expression and ^{18}F-FES uptake and the lack of changes in tumor cell proliferation (Ki-67 staining) and metabolism (^{18}F-FDG uptake), which were not yet apparent after fulvestrant treatment, at least up to 48 hours post-treatment (the time point evaluated in the current study). This is in contrast to the results from clinical studies indicating that ER, and the cell proliferation marker, Ki-67, were downregulated with fulvestrant treatment (13, 14, 37). We used similar doses of fulvestrant given in widespread reports in similar preclinical tumor model (31, 38, 39). However, in our study, the time between treatment and tumor extraction was much shorter than previous reports and was likely insufficient for ER degradation to affect subsequent downstream metabolic and proliferation pathways. This represents a unique advantage for ^{18}F-FES in identifying early pharmacodynamic changes and demonstrates how imaging steroid hormone receptors can be used for dose optimization of fulvestrant based on functional, unoccupied ER measurements. Thus, ^{18}F-FES could be a better surrogate for optimized fulvestrant dosing in individuals with BrCa compared to other noninvasive assessments such as tumoral ^{18}F-FDG uptake. Such personalized treatment may provide additional benefit over standard uniform dosing approaches currently employed and allows for early alternative intervention for nonresponsive tumors.

There are several limitations to this study. First, endocrine therapies that directly block ER (e.g., fulvestrant, tamoxifen, and raloxifene) or diminish ER protein levels (e.g., fulvestrant) both can decrease the ^{18}F-FES uptake by tumor. Thus, it is not possible to determine what proportion of change in ^{18}F-FES uptake is due to either effect. Second, measuring receptor occupancy levels using ^{18}F-FES PET is most useful when the receptor-targeted therapies such as tamoxifen or fulvestrant is in the subsaturating range. If the administered dose of anti-estrogen is high enough to completely saturate receptors, then there will be no receptor-specific tracer uptake; in these circumstances, receptor quantitation using PET imaging shows complete occupancy and the degree of excess drug dose cannot be assessed. In practice, the majority of BrCa patients is given subsaturating doses of anti-ER therapy and

may benefit from dose adjustment using the proposed approach. Third, the data presented in this study are derived from experiments on a well-established model of ER+ BrCa that is commonly used. Using this model we demonstrated the feasibility of pharmacodynamic imaging for improved fulvestrant dosing. However, since the model we utilized was only derived from MCF-7 cells, generalizing these findings may require further studies with multiple BrCa models.

This study provides preliminary evidence that responsiveness to endocrine therapy could be measured early in the course of ER-targeting therapies by quantitative imaging of ER binding in BrCa. In this regard, serial ^{18}F-FES PET imaging provides a quantitative assessment of changes in receptor binding caused by therapeutics aimed to induce receptor blockade/degradation, and thus has the potential to refine treatment selection and dosing in individual patients. In particular, ^{18}F-FES PET could notify the oncologist early in the course of treatment of inadequate anti-ER therapy and guide improved dosing of anti-ER therapeutics. This technology could also be used early in drug development to measure effectiveness at the intended therapeutic targets and to help refine patient selection and dosing levels for agents in drug development. In addition, this image-guided approach to individualized drug dosing may also be employed for other receptor-targeted therapies in cancer treatment in the future. Given the limitations of this study, further study using carefully timed serial ^{18}F-FES imaging is warranted to assess the role for this imaging tool in ER-targeted therapies in the clinical setting.

Acknowledgments

Financial support: This research was supported in part by National Institutes of Health grants U01CA084301 and P50CA127003.

This work was supported by U01CA084301 and P50CA127003. Francis Deng supported by a Bradley-Alavi Student Fellowship from the Society for Nuclear Medicine and Molecular Imaging and a Washington University School of Medicine Dean's Fellowship. We thank Anna Levitz, MGH Specialized Histopathology Services, and Caitlin Routhier, MGH Immunopathology Unit, for technical assistance with IHC. We also thank Bryan Chang for helpful discussions and technical assistance with maintaining tumor-bearing mice, and Nazife Selcan Turker for technical assistance with radiotracer administration.

References

1. Dunnwald LK, Rossing MA, Li CI. Hormone receptor status, tumor characteristics, and prognosis: a prospective cohort of breast cancer patients. Breast Cancer Res. 2007; 9:R6. [PubMed: 17239243]
2. Li CI, Daling JR, Malone KE. Incidence of invasive breast cancer by hormone receptor status from 1992 to 1998. J Clin Oncol. 2003; 21:28–34. [PubMed: 12506166]
3. Osborne CK, Yochmowitz MG, Knight WA 3rd, McGuire WL. The value of estrogen and progesterone receptors in the treatment of breast cancer. Cancer. 1980; 46:2884–8. [PubMed: 7448733]
4. Nicholson RI, Bouzubar N, Walker KJ, McClelland R, Dixon AR, Robertson JF, et al. Hormone sensitivity in breast cancer: influence of heterogeneity of oestrogen receptor expression and cell proliferation. Eur J Cancer. 1991; 27:908–13. [PubMed: 1834127]
5. Osborne CK. Heterogeneity in hormone receptor status in primary and metastatic breast cancer. Semin Oncol. 1985; 12:317–26. [PubMed: 3901267]
6. Long X, Nephew KP. Fulvestrant (ICI 182,780)-dependent interacting proteins mediate immobilization and degradation of estrogen receptor-alpha. J Biol Chem. 2006; 281:9607–15. [PubMed: 16459337]

7. Nawaz Z, Lonard DM, Dennis AP, Smith CL, O'Malley BW. Proteasome-dependent degradation of the human estrogen receptor. Proc Natl Acad Sci U S A. 1999; 96:1858–62. [PubMed: 10051559]
8. Dauvois S, White R, Parker MG. The antiestrogen ICI 182780 disrupts estrogen receptor nucleocytoplasmic shuttling. J Cell Sci. 1993; 106 (Pt 4):1377–88. [PubMed: 8126115]
9. Howell A, Robertson JF, Quaresma Albano J, Aschermannova A, Mauriac L, Kleeberg UR, et al. Fulvestrant, formerly ICI 182,780, is as effective as anastrozole in postmenopausal women with advanced breast cancer progressing after prior endocrine treatment. J Clin Oncol. 2002; 20:3396–403. [PubMed: 12177099]
10. Osborne CK, Pippen J, Jones SE, Parker LM, Ellis M, Come S, et al. Double-blind, randomized trial comparing the efficacy and tolerability of fulvestrant versus anastrozole in postmenopausal women with advanced breast cancer progressing on prior endocrine therapy: results of a North American trial. J Clin Oncol. 2002; 20:3386–95. [PubMed: 12177098]
11. Robertson JF, Llombart-Cussac A, Rolski J, Feltl D, Dewar J, Macpherson E, et al. Activity of fulvestrant 500 mg versus anastrozole 1 mg as first-line treatment for advanced breast cancer: results from the FIRST study. J Clin Oncol. 2009; 27:4530–5. [PubMed: 19704066]
12. Robertson JF. Fulvestrant (Faslodex) -- how to make a good drug better. Oncologist. 2007; 12:774–84. [PubMed: 17673609]
13. DeFriend DJ, Howell A, Nicholson RI, Anderson E, Dowsett M, Mansel RE, et al. Investigation of a new pure antiestrogen (ICI 182780) in women with primary breast cancer. Cancer Res. 1994; 54:408–14. [PubMed: 8275477]
14. Robertson JF, Nicholson RI, Bundred NJ, Anderson E, Rayter Z, Dowsett M, et al. Comparison of the short-term biological effects of 7alpha-[9-(4,4,5,5,5-pentafluoropentylsulfinyl)-nonyl]estra-1,3,5, (10)-triene-3,17beta-diol (Faslodex) versus tamoxifen in postmenopausal women with primary breast cancer. Cancer Res. 2001; 61:6739–46. [PubMed: 11559545]
15. Ohno S, Rai Y, Iwata H, Yamamoto N, Yoshida M, Iwase H, et al. Three dose regimens of fulvestrant in postmenopausal Japanese women with advanced breast cancer: results from a double-blind, phase II comparative study (FINDER1). Ann Oncol. 2010; 21:2342–7. [PubMed: 20494961]
16. Pritchard KI, Rolski J, Papai Z, Mauriac L, Cardoso F, Chang J, et al. Results of a phase II study comparing three dosing regimens of fulvestrant in postmenopausal women with advanced breast cancer (FINDER2). Breast Cancer Res Treat. 2010; 123:453–61. [PubMed: 20632084]
17. Di Leo A, Jerusalem G, Petruzelka L, Torres R, Bondarenko IN, Khasanov R, et al. Results of the CONFIRM phase III trial comparing fulvestrant 250 mg with fulvestrant 500 mg in postmenopausal women with estrogen receptor-positive advanced breast cancer. J Clin Oncol. 2010; 28:4594–600. [PubMed: 20855825]
18. Garnett SA, Martin M, Jerusalem G, Petruzelka L, Torres R, Bondarenko IN, et al. Comparing duration of response and duration of clinical benefit between fulvestrant treatment groups in the CONFIRM trial: application of new methodology. Breast Cancer Res Treat. 2013; 138:149–55. [PubMed: 23378064]
19. Heidari P, Wehrenberg-Klee E, Habibollahi P, Yokell D, Kulke M, Mahmood U. Free somatostatin receptor fraction predicts the antiproliferative effect of octreotide in a neuroendocrine tumor model: implications for dose optimization. Cancer Res. 2013; 73:6865–73. [PubMed: 24080280]
20. McGuire AH, Dehdashti F, Siegel BA, Lyss AP, Brodack JW, Mathias CJ, et al. Positron tomographic assessment of 16 alpha-[^{18}F] fluoro-17 beta-estradiol uptake in metastatic breast carcinoma. J Nucl Med. 1991; 32:1526–31. [PubMed: 1869973]
21. Mortimer JE, Dehdashti F, Siegel BA, Katzenellenbogen JA, Fracasso P, Welch MJ. Positron emission tomography with 2-[^{18}F]Fluoro-2-deoxy-D-glucose and 16alpha-[^{18}F]fluoro-17beta-estradiol in breast cancer: correlation with estrogen receptor status and response to systemic therapy. Clin Cancer Res. 1996; 2:933–9. [PubMed: 9816253]
22. Sundararajan L, Linden HM, Link JM, Krohn KA, Mankoff DA. ^{18}F-Fluoroestradiol. Semin Nucl Med. 2007; 37:470–6. [PubMed: 17920354]
23. Dehdashti F, Mortimer JE, Siegel BA, Griffeth LK, Bonasera TJ, Fusselman MJ, et al. Positron tomographic assessment of estrogen receptors in breast cancer: comparison with FDG-PET and in vitro receptor assays. J Nucl Med. 1995; 36:1766–74. [PubMed: 7562040]

24. Peterson LM, Mankoff DA, Lawton T, Yagle K, Schubert EK, Stekhova S, et al. Quantitative imaging of estrogen receptor expression in breast cancer with PET and ^{18}F-fluoroestradiol. J Nucl Med. 2008; 49:367–74. [PubMed: 18287268]
25. Peterson LM, Kurland BF, Schubert EK, Link JM, Gadi VK, Specht JM, et al. A Phase 2 Study of 16alpha-[F]-fluoro-17beta-estradiol Positron Emission Tomography (FES-PET) as a Marker of Hormone Sensitivity in Metastatic Breast Cancer (MBC). Mol Imaging Biol. 2013 In press.
26. Currin E, Linden HM, Mankoff DA. Predicting Breast Cancer Endocrine Responsiveness Using Molecular Imaging. Curr Breast Cancer Rep. 2011; 3:205–11. [PubMed: 23105956]
27. Linden HM, Stekhova SA, Link JM, Gralow JR, Livingston RB, Ellis GK, et al. Quantitative fluoroestradiol positron emission tomography imaging predicts response to endocrine treatment in breast cancer. J Clin Oncol. 2006; 24:2793–9. [PubMed: 16682724]
28. Dehdashti F, Mortimer JE, Trinkaus K, Naughton MJ, Ellis M, Katzenellenbogen JA, et al. PET-based estradiol challenge as a predictive biomarker of response to endocrine therapy in women with estrogen-receptor-positive breast cancer. Breast Cancer Res Treat. 2009; 113:509–17. [PubMed: 18327670]
29. Linden HM, Kurland BF, Peterson LM, Schubert EK, Gralow JR, Specht JM, et al. Fluoroestradiol positron emission tomography reveals differences in pharmacodynamics of aromatase inhibitors, tamoxifen, and fulvestrant in patients with metastatic breast cancer. Clin Cancer Res. 2011; 17:4799–805. [PubMed: 21750198]
30. Lim JL, Zheng L, Berridge MS, Tewson TJ. The use of 3-methoxymethyl-16 beta, 17 beta-epiestriol-O-cyclic sulfone as the precursor in the synthesis of F-18 16 alpha-fluoroestradiol. Nucl Med Biol. 1996; 23:911–5. [PubMed: 8971859]
31. Fowler AM, Chan SR, Sharp TL, Fettig NM, Zhou D, Dence CS, et al. Small-animal PET of steroid hormone receptors predicts tumor response to endocrine therapy using a preclinical model of breast cancer. J Nucl Med. 2012; 53:1119–26. [PubMed: 22669982]
32. Kuter I, Gee JM, Hegg R, Singer CF, Badwe RA, Lowe ES, et al. Dose-dependent change in biomarkers during neoadjuvant endocrine therapy with fulvestrant: results from NEWEST, a randomized Phase II study. Breast Cancer Res Treat. 2012; 133:237–46. [PubMed: 22286314]
33. van Kruchten M, de Vries EG, Brown M, de Vries EF, Glaudemans AW, Dierckx RA, et al. PET imaging of oestrogen receptors in patients with breast cancer. Lancet Oncol. 2013; 14:e465–75. [PubMed: 24079874]
34. van Kruchten, M.; De Vries, E.; Brown, M.; Glaudemans, AWJM.; van Lanschot, MC.; Kema, IP., et al. Residual estrogen receptor availability during fulvestrant 500 mg therapy in patients with metastatic breast cancer. ASCO Annual Meeting; 2014; 2014. p. 588
35. Du X, Li XQ, Li L, Xu YY, Feng YM. The detection of ESR1/PGR/ERBB2 mRNA levels by RT-QPCR: a better approach for subtyping breast cancer and predicting prognosis. Breast Cancer Res Treat. 2013; 138:59–67. [PubMed: 23397283]
36. Pentheroudakis G, Kotoula V, Eleftheraki AG, Tsolaki E, Wirtz RM, Kalogeras KT, et al. Prognostic significance of ESR1 gene amplification, mRNA/protein expression and functional profiles in high-risk early breast cancer: a translational study of the Hellenic Cooperative Oncology Group (HeCOG). PLoS One. 2013; 8:e70634. [PubMed: 23923010]
37. Mankoff DA, Dehdashti F, Shields AF. Characterizing tumors using metabolic imaging: PET imaging of cellular proliferation and steroid receptors. Neoplasia. 2000; 2:71–88. [PubMed: 10933070]
38. Brodie A, Jelovac D, Long BJ. Predictions from a preclinical model: studies of aromatase inhibitors and antiestrogens. Clin Cancer Res. 2003; 9:455S–9S. [PubMed: 12538500]
39. Hoffmann J, Bohlmann R, Heinrich N, Hofmeister H, Kroll J, Kunzer H, et al. Characterization of new estrogen receptor destabilizing compounds: effects on estrogen-sensitive and tamoxifen-resistant breast cancer. J Natl Cancer Inst. 2004; 96:210–8. [PubMed: 14759988]

TRANSLATIONAL RELEVANCE

Fulvestrant, a selective estrogen receptor degrader, is approved for treatment of ER positive metastatic BrCa in postmenopausal women. The optimal dosing has been an area for debate; the lower than expected clinical performance in BrCa may be partially explained by inadequate fulvestrant dosing. This study provides evidence that responsiveness to anti-ER therapies such as fulvestrant could be measured by early pharmacodynamic imaging of ER binding/degradation. We demonstrate that ^{18}F-FES uptake mirrors the dose-dependent changes in functional ER expression with fulvestrant treatment, which precedes the changes in tumor metabolism and proliferation. Therefore, ^{18}F-FES PET could be employed early in treatment to guide improved dosing of anti-ER therapeutics. This technology could also be used in drug development to measure effectiveness at the intended therapeutic targets, to help refine patient selection and dosing levels for agents in clinical trials. Moreover, this approach may be employed for other receptor-targeted therapies in cancer treatment.

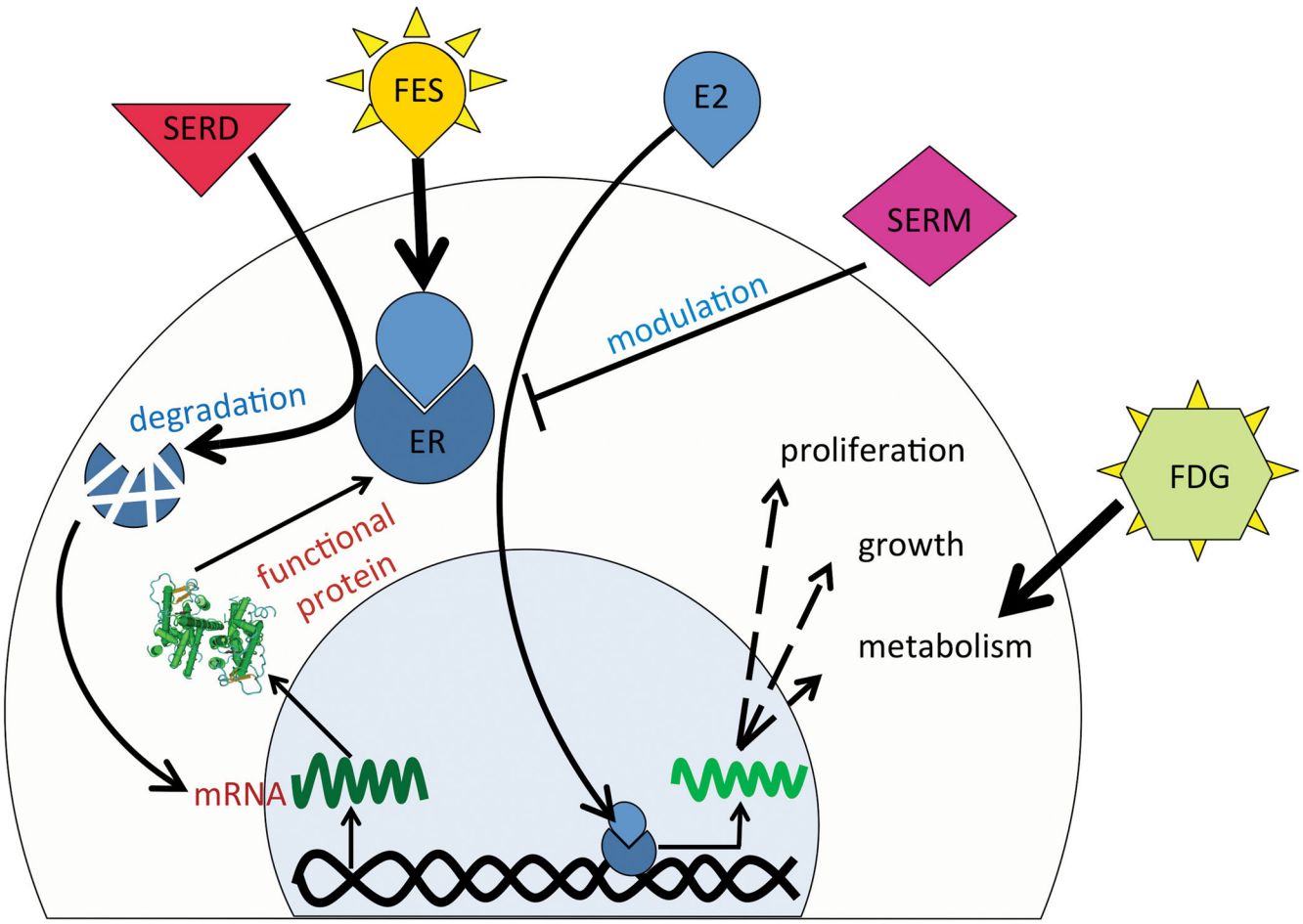

Figure 1.

Schematic representation of ER kinetics in BrCa cells, effect of ER-targeted therapeutics, and interaction of commonly used PET tracers with BrCa cells. ER binds estradiol (E2) and after translocation to the cell nucleus enhances cell growth, metabolism and proliferation, which in turn results in increased ^{18}F-FDG uptake by cancer cells. SERMs through blocking ER and SERDs by degrading ER reduce cell growth. Enhanced ER mRNA transcription and translation, due to relief of a negative feedback loop, may eventually compensate the decrease in functional ER molecules. The level of available functional ER can be quantified using the PET tracer ^{18}F-FES.

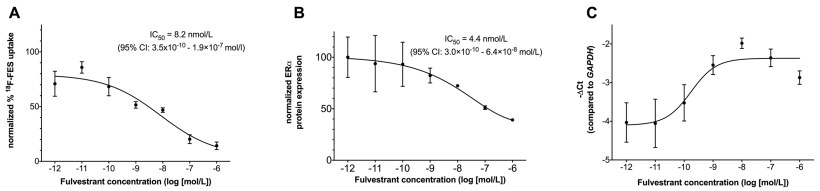

Figure 2.

In vitro experiments. In all experiments MCF7 cells were treated with fulvestrant for 24 hours. The results were normalized to an ER-negative control cell line, MDA-MB-231. (A) ^{18}F-FES retention is plotted against fulvestrant concentration (log [mol/L]). The ^{18}F-FES uptake gradually decreases with increasing dose of fulvestrant (ANOVA p=0.0005). Data are triplicate samples. Results were radioactive decay-corrected. (B) ERα expression determined by sandwich ELISA in MCF-7 cells treated with a range of fulvestrant concentrations (log [mol/L]). Data are from biological replicates in two independent experiments and normalized to MDA-MB-231. (C) *ESR1* mRNA expression versus fulvestrant concentration as determined by qRT-PCR. Results displayed are average cycle threshold (Ct) for *ESR1* subtracted from that of the housekeeping gene *GAPDH* for each group. −ΔCt approximates the base-2 logarithm of relative gene expression. Data are from biological replicates in two independent experiments. Error bars are SEM.

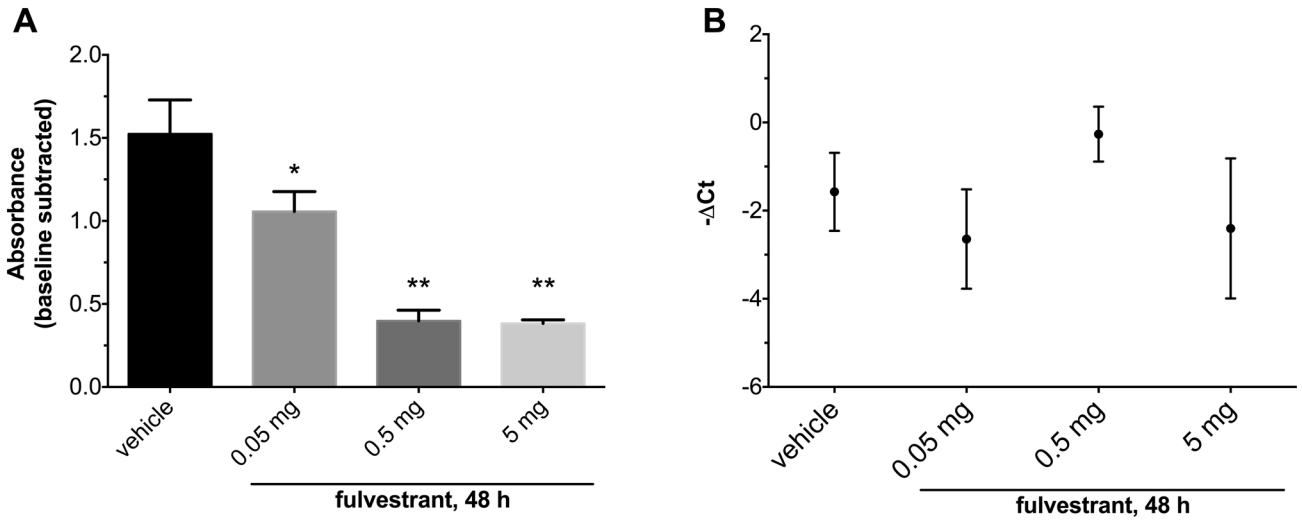

Figure 3.

Ex vivo analyses of MCF7 xenografts. Nude mice bearing MCF7 xenografts were given one dose of fulvestrant 48 h before tumors were extracted for analysis (n=2–3 mice per group). (A) ERα expression versus fulvestrant dose as determined by sandwich ELISA. Means were compared to vehicle control. There was a significant reduction in ERα expression level with fulvestrant treatment (ANOVA p=0.001). The reduction in ERα expression was more pronounced with higher doses of fulvestrant. (B) *ESR1* mRNA expression versus fulvestrant dose as determined by qRT-PCR. There was no significant difference among treatment groups in ERα mRNA expression. *p<0.05, **p<0.01. Error bars are SEM.

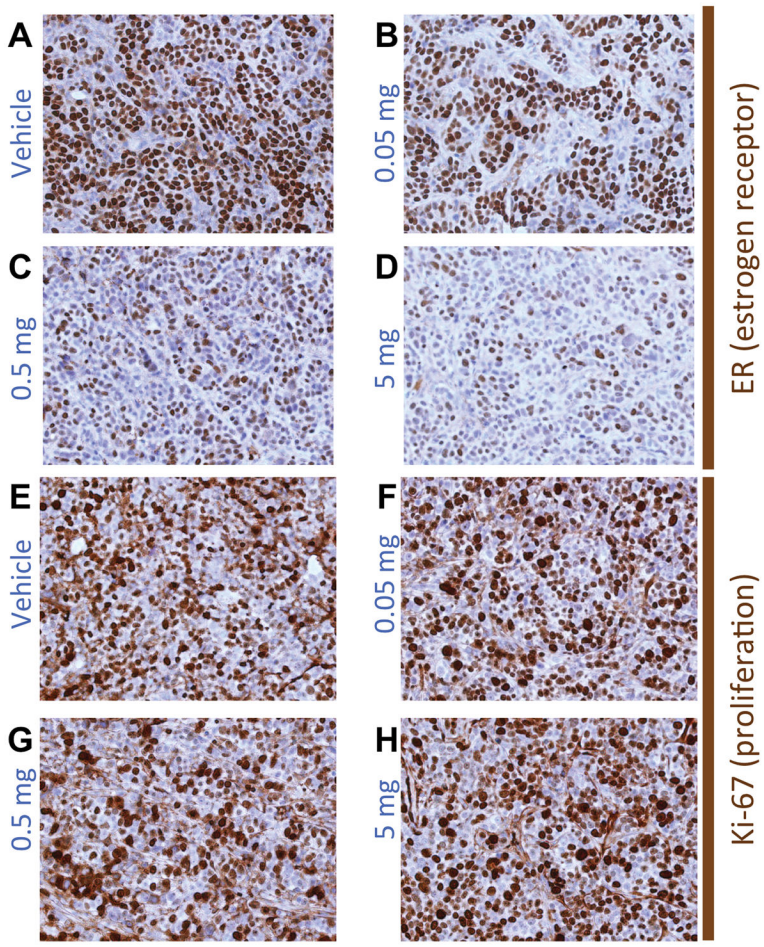

Figure 4.

(A–D) Representative IHC for ER and (E–H) for the proliferation marker Ki-67, corresponding to MCF-7 xenografts from mice treated with one dose of (A,E) vehicle, (B,F) 0.05 mg,(C,G) 0.5 mg, or (D,H) 5 mg fulvestrant. The number of cells and the intensity of staining for ER monotonically diminish with increased doses of fulvestrant while the Ki-67 staining remained relatively constant among treatment groups across all doses.

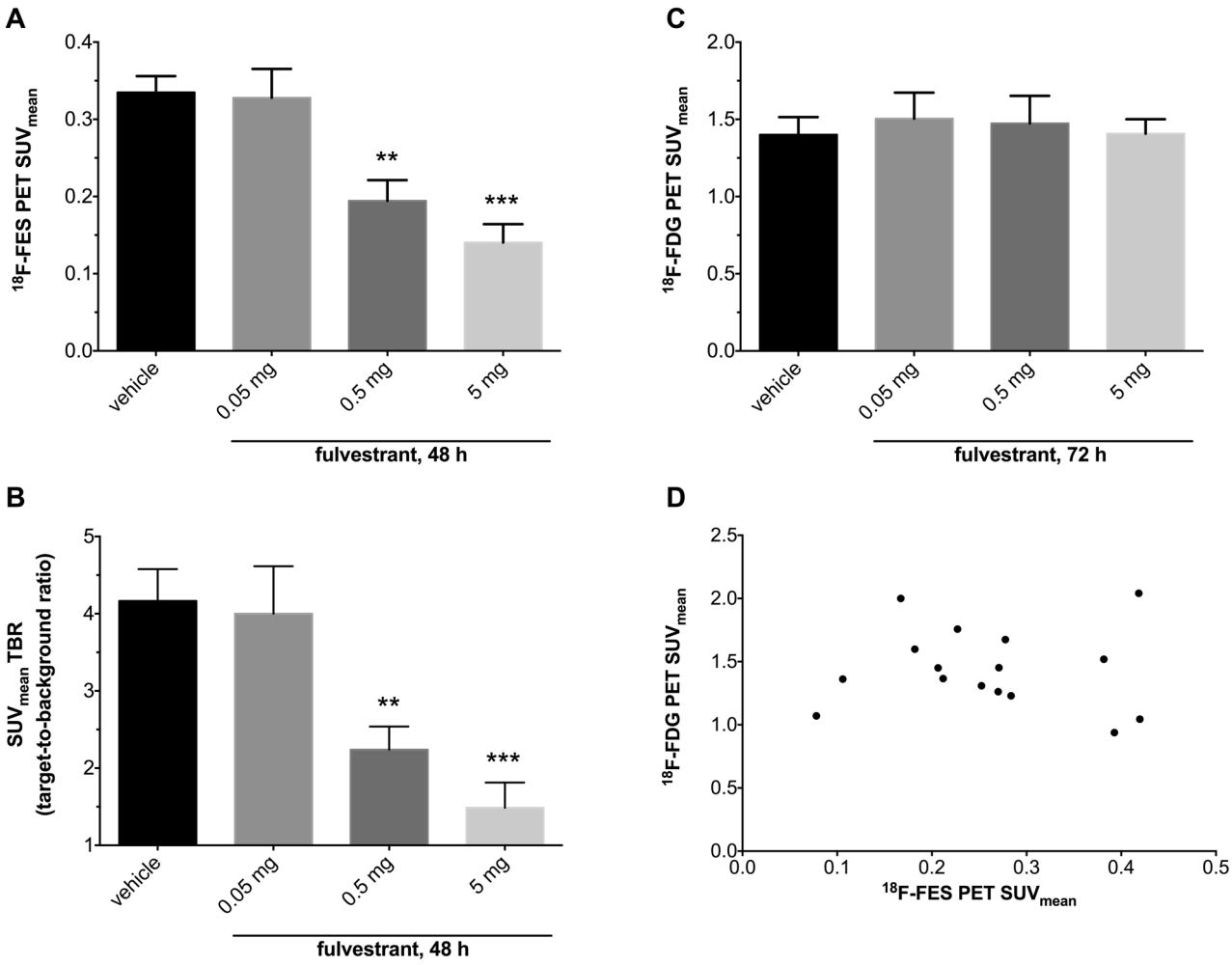

Figure 5.

Quantitative in vivo imaging. Mean standardized uptake values (SUV_{mean}) (A) and target-to-background ratio (TBR) (B) of xenografts in ^{18}F-FES PET scans 48 hours after fulvestrant treatment. There was a significant reduction in ^{18}F-FES SUV_{mean} and TBR with fulvestrant treatment (ANOVA p=0.0001). Holm-Sidak's multiple comparison test revealed decreased uptake in intermediate and high dose groups compared to vehicle control. (C) ^{18}F-FDG PET scans performed 24 hours after ^{18}F-FES PET did not reveal any difference in SUV_{mean} of xenografts among treatment groups (ANOVA p=0.94); (D) Pearson correlation between SUV_{mean} from serial FES and FDG PET on select mice showing essentially no correlation between two scans (n=3–5/group, R^2=0.0014, P=0.89). n=5–6 mice per group; **p<0.01, ***p<0.001; n=5–6 mice per group. Error bars are SEM.

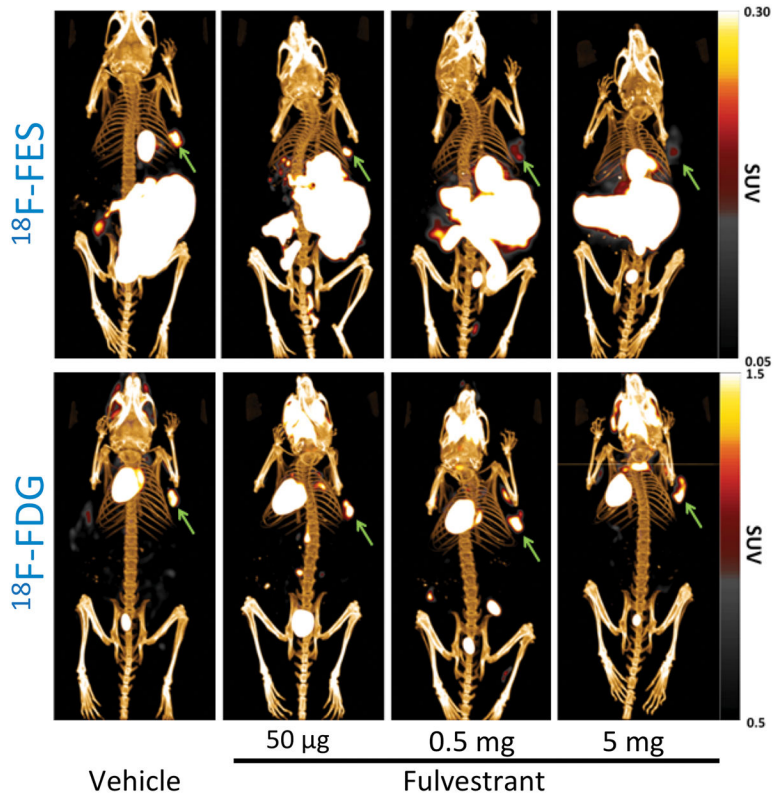

Figure 6.

Posterior 3D volume rendering of fused PET/CT scans of mice bearing breast tumors in the upper right flank and treated with fulvestrant. Upper panel: ^{18}F-FES PET representative images. ^{18}F-FES uptake decreases in xenografts with increased dose of fulvestrant. The gallbladder and bowel show high uptake consistent with hepatobiliary excretion of ^{18}F-FES. Lower panel: ^{18}F-FDG PET representative images. There is no difference among groups in ^{18}F-FDG uptake. Green arrows indicate tumor.